American Mineralogist, Volume 103, pages 1711–1715, 2018

New Mineral Names*,†

Dmitriy I. Belakovskiy[1] and Olivier C. Gagné[2]

[1]Fersman Mineralogical Museum, Russian Academy of Sciences, Leninskiy Prospekt 18 korp. 2, Moscow 119071, Russia
[2]Department of Geological Sciences, University of Manitoba, Winnipeg, Manitoba R3T 2N2, Canada

In this issue

This New Mineral Names has entries for eight new minerals, including abellaite, babánekite, delhuyarite-(Ce), murakamiite, oxy-foitite, shenzhuangite, siidraite, and ulfanderssonite-(Ce).

Abellaite*

J. Ibáñez-Insa, J.J. Elvira, X. Llovet, J. Pérez-Cano, N. Oriols, M. Busquets-Masó, and S. Hernández (2017) Abellaite, $NaPb_2(CO_3)_2(OH)$, a new supergene mineral from the Eureka mine, Lleida province, Catalonia, Spain. European Journal of Mineralogy, 29(5), 915–922.

Abellaite (IMA 2014-111), ideally $NaPb_2(CO_3)_2(OH)$, is a new mineral from the abandoned Eureka uranium mine (42°23′10″N, 0°57′27″E), in the southern Pyrenees (Lleida province), Catalonia, Spain. The primary U–V–Cu mineralization is hosted within the fluvial continental Buntsandstein redbeds and represented by millimeter-sized grains of various sulfides, sulfosalts, selenides, U–V oxides, silicates containing Cu, V, U, Bi, Ag, Se, As, Ni, and Co. Abellaite is a post-mining secondary mineral that resulted of supergene enrichment. It forms sparse coatings most often on a substrate of quartzite, in association with primary minerals (roscoelite, pyrite, uraninite, coffinite, carbon, galena, sphalerite, native bismuth, Ni-rich cobaltite, covellite, tennantite, and chalcopyrite), and supergene minerals (hydrozincite, aragonite, gordaite, As-vanadinite, andersonite, čejkaite, malachite, and devilline). In general, the mineral forms subhedral microcrystals not larger than 10 μm, but some larger (10–30 μm) idiomorphic, pseudohexagonal crystals with a prominent pinacoid face (and more poorly developed prism faces) have been observed. The more euhedral microcrystals have a tabular to lamellar habit and form disordered aggregates. Abellaite aggregates are colorless to white. Crystals are translucent with a vitreous to nacreous luster and a white streak. Abellaite does not show fluorescence under UV radiation. It is not soluble in water, but incongruently dissolve in 20% HCl at room temperature with separation of $PbCl_2$. Due to the small crystal size the cleavage, fracture, hardness, and density were not determined; D_{calc} = 5.93 g/cm^3. The synthetic analog of abellaite has a perfect cleavage on {001}. For the same reason most of optical properties were not obtained. The mineral is non-pleochroic and refractive indexes are estimated to be between 1.8 and 2; n_{calc} = 1.90. The Raman spectrum shows a sharp band at ~1058 cm^{-1} and a weaker, broader feature at ~1391 cm^{-1}, which can be attributed to symmetric (ν_1) and asymmetric (ν_3) stretching modes of CO_3^{2-} groups, respectively. A weak peak is observed at 3504 cm^{-1}, is assigned to O–H stretching vibrations. The main absorption bands of the IR spectrum (cm^{-1}, w = weak, m = medium, s = strong, vs = very strong, br = broad) are: 688s [ν_4 (CO_3^{2-})], 844m [ν_2 (CO_3^{2-})], 998w,br (δPbOH), 1053w [ν_1 (CO_3^{2-})], 1425vs,br [ν_3 (CO_3^{2-})], 1750w,br (second order), 3500w,br (O-H stretching). The average of 10 electron probe WDS analyses is [wt% (range)]: Na 3.88 (3.69–4.03), Ca 0.29 (0.14–0.51), Pb 72.03 (71.14–72.7), C 4.17, O 19.47, H 0.17, total 100.01. H, C, and O were determined by stoichiometry. This gives the empirical formula $Na_{0.96}Ca_{0.04}Pb_{1.98}(CO_3)_2(OH)$ based on 7 O pfu. The strongest lines in the X-ray powder-diffraction pattern [*d* Å (*I*%; *hkl*)] are: 3.193 (100; 013), 2.627 (84; 110), 2.275 (29; 020), 2.242 (65; 021,006), 2.029 (95; 023). Single-crystal X-ray diffraction data was not done due to the mineral being too fine grained. Rietveld refinements using crystallographic data for synthetic analog of abellaite as a starting model show the mineral is hexagonal, space group $P6_3mc$, a = 5.254(2), c = 13.450(5) Å, V = 321.5 Å^3, Z = 2. Abellaite is named after the amateur mineralogist and mineral collector Joan Abella i Creus (b. 1968) from Sabadell, Catalonia, Spain, who collected the mineral. Co-type material is deposited in the Natural History Museum of Barcelona, Catalonia, Spain. **O.C.G.**

Babánekite*

J. Plášil, P. Škácha, J. Sejkora, R. Škoda, M. Novák, F. Veselovský, and J. Hloušek (2017) Babánekite, $Cu_3(AsO_4)_2{\cdot}8H_2O$, from Jáchymov, Czech Republic—a new member of the vivianite group. Journal of Geosciences, 62 (4), 261–270.

Babánekite (IMA 2012-007), ideally $Cu_3(AsO_4)2{\cdot}8H_2O$, monoclinic, is a new member of the vivianite group $Me_3(XO_4)_2(H_2O)_8$ where *Me* = divalent cations and $X = P^{5+}$ or As^{5+}. Four P-dominant members [vivianite (Fe), arupite (Ni), barićite (Mg, Fe), and pakhomovskyite (Co)] and six As-dominant members [annabergite (Ni), erythrite (Co), hörnesite (Mg), manganohörnesite (Mn), köttigite (Zn), and parasymplesite (Fe)] of this group were known to date. The new member was found in an old ore-stope (so called "lindackerite stope") on the Geister vein at the third Geister level of the Rovnost (former Werner) mine, Jáchymov, Western Bohemia, Czech Republic. The Jáchymov ore district represents a classic example of Ag–As–Bi–Co–Ni–U hydrothermal vein-type deposit. Babánekite was found in a supergene oxidation zone in a rich association constituted by arsenates of the vivianite group and lindackerite supergroup, as well as supergene uranyl-bearing minerals. The richness of the locality results from the occurrence of both the recently/sub-recently formed minerals connected with the post-mining processes and the supergene minerals formed in-situ in the oxidation zone (association of uranyl arsenates and vanadates; association of Pb–Cu supergene minerals and minerals containing Y+REE). Babánekite aggregates grow in cavities and on the surface of ore fragments closely associating with members of the lindackerite supergroup (lindackerite, veselovskýite, hloušekite, pradetite, and klajite), lavendulan, gypsum, and an X-ray amorphous Cu–Al–Si–O–H phase. These minerals crystallize on the strongly altered ore-body consisting mainly of massive tennantite, galena and chalcopyrite with disseminated uraninite in quartz. Babánekite crystals are pinkish to peach-colored, elongated, and prismatic up to 1.5 mm in length. They grouped in hemispherical aggregates up to 2 mm. Crystal forms are: {010}, {100}, {110}, {101}, and less frequently {001}. The mineral has a light pinkish streak and is transparent to translucent with

* All minerals marked with an asterisk have been approved by the IMA CNMMC.
† For a complete listing of all IMA-validated unnamed minerals and their codes, see http://pubsites.uws.edu.au/ima-cnmnc/.

0003-004X/18/0010–1711$05.00/DOI: https://doi.org/10.2138/am-2018-NMN1031020

a vitreous luster. The cleavage is perfect on {010}. Estimated Mohs hardness is 1½–2½ by analogy with other group members. Babánekite did not show any fluorescence under short- or long-wave UV radiation. Density was not measured due to paucity of pure material, D_{calc} = 3.192 g/cm^3. Optical properties were not determined referring to zonation of the available crystals; n_{calc} = 1.662. The average of 11 electron-probe WDS analysis [wt% (range)] is CoO 8.89 (6.49–10.65), NiO 4.06 (1.20–6.26), CuO 15.31 (10.72–20.01), ZnO 10.87 (8.70–14.51), P_2O_5 0.16 (0.10–0.24), As_2O_5 39.79 (39.01–40.58), SO_3 0.13 (0–0.37), H_2O (by stoichiometry) 24.78, total 103.99. Other elements concentrations were below detection limits. The empirical formula based on 16 O apfu is $(Cu_{1.12}Zn_{0.78}Co_{0.69}Ni_{0.32})_{\Sigma 2.91}[(AsO_4)_{2.01}(PO_4)_{0.01}(SO_4)_{0.01}]_{\Sigma 2.03}\cdot 8H_2O$. Crystals are zonal with Cu^{2+} content correlates negatively both with Ni^{2+} and Co^{2+}, but not with Zn^{2+}. Other samples of babánekite from Geister differ significantly having lower Zn^{2+} contents (not exceed 0.14 Zn pfu), along with the even more dominating Cu^{2+} (up to 1.78 Cu pfu). The strongest lines of the X-ray powder diffraction pattern are [*d* Å (*I*%; *hkl*)]: 7.936 (11; 110), 6.743 (100; 020), 3.231 (14; 13$\bar{1}$), 2.715 (11; 041), 2.333 (10; 15$\bar{1}$), 2.082 (5; 350), 1.686 (16; 080), 1.611 (4; 55$\bar{1}$). The unit-cell parameters refined from the powder data are a = 10.1850(6), b = 13.4852(6), c = 4.7484(3) Å, β = 105.316(5)°, V = 629.01 Å^3. The single-crystal X-ray data obtained from the crystal of 0.097 × 0.037 × 0.034 mm in size shows babánekite is monoclinic, *C*2/*m*, with a = 10.1729(3), b = 13.5088(4), c = 4.7496(1) Å, β = 105.399(2)°, V = 629.28 Å^3, Z = 2. The crystal structure of babánekite, refined to R_1 = 2.18 % for 864 unique observed reflections, confirmed to be similar to other members of the vivianite group where of $Me1O_2(H_2O)_4$ octahedra and dimers of $Me2_2O_6(H_2O)_4$ octahedra that are linked via XO_4 tetrahedra and hydrogen bonds to form complex layers parallel to (010). Adjacent layers are linked by hydrogen bonds only. The mineral is named for Senior Mining Counselor ("Oberbergrath") Ing. František Babánek (1836–1910), Czech mining expert, geologist and mineralogist who worked in the Jáchymov and Příbram mines. The type specimen is deposited in the Department of Mineralogy and Petrology of the National Museum, Prague, Czech Republic. **D.B.**

DELHUYARITE-(CE)*

D. Holstam, L. Bindi, U. Hålenius, and U.B. Anderson (2017) Delhuyarite-(Ce)—$Ce_4Mg(Fe_2^{3+}W)\square(Si_2O_7)_2O_6(OH)_2$—a new mineral of the chevkinite group, from the Nya Bastnäs Fe–Cu–REE deposit, Sweden. European Journal of Mineralogy, 29(5), 897–905.

Delhuyarite-(Ce) (IMA 2016-091), ideally $Ce_4Mg(Fe_2^{3+}W)\square(Si_2O_7)_2O_6(OH)_2$ monoclinic, is a new member of the chevkinite group discovered in the only known old museum specimen #NRM 19060375 from the Swedish Museum of Natural History, Sweden. This specimen is considered as holotype and is also the holotype for percleveite-(Ce). It was found at the Nya Bastnäs Fe–Cu–REE mines (Riddarhyttan ore field), Skinnskatteberg, Västmanland, Sweden (59°50′47″N, 15°35′15″E, 220 m a.s.l.). This deposit is famous for being the type locality for more than 20 REE mineral species including cerite-(Ce), bastnäsite-(Ce), and others. At the deposit, quartz-banded hematite ore occurs in proximity with a magnetite-skarn ore, the latter replacing a dolomitic carbonate horizon. The dominant host rock is a quartz-rich, cordierite-bearing mica-schist, interpreted as an extensively metasomatized (Mg–K alteration) and regionally metamorphosed (amphibolite facies) felsic volcanogenic unit originally deposited at ~1.9 Ga. Identified associated minerals are cerite-(Ce), tremolite-actinolite, bastnäsite-(Ce), magnetite, quartz, chalcopyrite, ferriallanite-(Ce), törnebohmite-(Ce), and scheelite. The late-formed quartz appears in interstices and microcracks in the REE-mineral assemblage. Delhuyarite-(Ce) forms brown–black translucent subhedral crystals up to 0.3 × 0.06 mm appearing essentially isolated in a mass of cerite-(Ce) and percleveite-(Ce). It has a dark brown streak, an adamantine luster, irregular to sub-conchoidal fracture, and no cleavage. Mohs hardness is estimated as 5–6, by analogy with chevkinite-group minerals. The density was not measured due to the minute size and the paucity of the material; D_{calc} = 5.196 g/cm^3. Delhuyarite-(Ce) is strongly pleochroic from rust-red to nearly opaque. It is optically biaxial (–). The strong absorption and high refraction did not allow to determine refractive indexes and other optical properties, n_{calc} = 1.94. The average of four point electron-probe WDS analyses [wt% (range)] is La_2O_3 14.58 (13.70–15.06), Ce_2O_3 23.29 (23.14–23.40), Pr_2O_3 1.89 (1.84–1.94), Nd_2O_3 6.13 (5.96–6.34), Sm_2O_3 0.74 (0.67–0.82), Gd_2O_3 0.37 (0.31–0.40), Dy_2O_3 0.03 (0–0.09), Er_2O_3 0.04 (0–0.06), Yb_2O_3 0.12 (0–0.06), Y_2O_3 0.22 (0.10–0.17), CaO 0.76 (0.69–0.93), Fe_2O_3 12.86 (12.23–14.11) (considered to be all trivalent based on bond distances and charge balance), MgO 2.43 (2.17–2.67), Al_2O_3 0.73 (0.50–0.88), SiO_2 18.16 (17.47–18.89), TiO_2 0.09 (0.07–0.12), WO_3 15.53 (15.21–16.01), F 0.05 (0.03–0.06), Cl 0.03 (0.02–0.03), H_2O_{calc} 1.33 (by structure based on 2 OH+F pfu), –O=F_2 0.02, –O=Cl_2 0.01, total 99.35. The Na, K, P, Sr, Ba, Mn, Th, U, Zr, Nb, Ho, and Lu contents were found to be below detection limits (<0.01 wt%). Concentration of Eu was not measured due to interference with other REE. An empirical formula based on 22 O is $(Ce_{1.89}La_{1.19}Nd_{0.48}Pr_{0.15}Sm_{0.06}Gd_{0.03}Y_{0.03}Ca_{0.18})_{\Sigma 4.01}(Fe^{3+}_{2.14}W_{0.89}Mg_{0.80}Al_{0.19}Ti_{0.02})_{\Sigma 4.04}Si_{4.01}O_{20}(OH_{1.96}F_{0.04})_{\Sigma 2}$. FTIR unpolarized single-crystal spectrum obtained in the range 2000–5000 cm^{-1} shows a strong absorption band at 3495 cm^{-1} confirming the presence of OH-groups. The strongest lines of the calculated X-ray powder diffraction pattern (based on single-crystal data for untreated crystal) are [d_{calc} Å (I_{calc}%; *hkl*)]: 10.808 (99; 001), 4.886 (43; 11$\bar{1}$), 4.611 (71; 111), 3.603 (48; 003), 3.211 (100; 311), 3.170 (66; 31$\bar{2}$), 3.113 (55; 40$\bar{2}$), 3.037 (71; 401), 2.872 (54; 020), 2.769 (53; 312), 2.726 (91; 31$\bar{3}$), 2.702 (83; 004). The single-crystal X-ray data were obtained on untreated crystal of 0.035 × 0.050 × 0.055 mm in size shows delhuyarite-(Ce) is monoclinic, space group *C*2/*m*, with unit-cell parameters a =13.6020(6), b = 5.7445(3), c = 10.9996(5)Å, β = 100.721(4)°, V = 844.47 Å^3, Z = 2. The unit-cell parameters for the annealed crystal (20 h in inert atmosphere at 800 °C) are a = 13.5559(5), b = 5.7023(2), c = 10.9485(4) Å, β = 100.481(4)°, V = 832.20 Å^3. The crystal structure was refined to R_1 = 3.9%. for an unheated crystal and to R_1 = 1.7% for 1213 unique $I > 2\sigma(I)$ reflections for an annealed crystal. Delhuyarite-(Ce) structure has the same topology as chevkinite subgroup minerals. There are two distinct rutile-like chains of octahedra ([M3+M4] and [M2+M2]) that extend in the **b** direction and link to form a layer of octahedra parallel to (001) with the insular M1 octahedra between the layers. The layers of octahedra link through [Si_2O_7] groups to form a framework with two interstitial *A* sites, in which Ce is dominant over other REE and Ca. It is the only mineral of the group with a significant content of W^{6+} = 0.89 apfu. In delhuyarite-(Ce), Mg is dominant at the M1 site as in polyakovite-(Ce); the composition of the M2, M3, and M4 sites is [$(Fe_2^{3+}W\square$], with M2 being 50% vacant. It has a high nominal H_2O content corresponding to one hydroxyl group and no Ti-dominated site. The name honors two mineral chemists and metallurgists, Juan José (1754–1796) and Fausto Fermín (1755–1833) de Elhuyar y de Lubice, brothers who first isolated tungsten metal in 1783. **D.B.**

MURAKAMIITE*

T. Imaoka, M. Nagashima, T. Kano, J.-I. Kimura, Q. Chang, and C. Fukuda (2017) Murakamiite, $LiCa_2Si_3O_8(OH)$, a Li-analog of pectolite, from the Iwagi Islet, southwest Japan. European Journal of Mineralogy, 29(6), 1045–1050.

Murakamiite (IMA 2016-066), ideally $LiCa_2Si_3O_8(OH)$, triclinic, is a new mineral and Li-analog of pectolite. It was discovered in an aegirine-augite albitite at the in the eastern part of Iwagi Islet, Ehime Prefecture, Japan (34.263°N, 133.161°E). The albitites hosted by Late Cretaceous biotite granitoids and consist of albite (~80 vol%), sugilite (~9%), aegirine-augite (~3%), quartz (~3%), pectolite (1%), orthoclase

(0.3%), and katayamalite (0.1%). Accessory minerals include zircon, britholite-(Ce), fluorapatite, titanite, and an unidentified Si–Th–Ca mineral. Murakamiite forms finely or coarsely prismatic, monomineralic aggregates up to 1.7 mm with representative grain sizes 0.2–0.3 mm, commonly in direct contacts with aegirine-albite. It is white to colorless with a white streak and a vitreous to silky luster. The mineral exhibits purplish-pink fluorescence under long-wave (365 nm) UV light. It is brittle with a splintery fracture and perfect cleavage on {100} and {001}. The Mohs hardness is 4½–5; D_{meas} = 2.86(1); D_{calc} =2.85 g/cm^3. Murakamiite is non-pleochroic, optically biaxial (+); α = 1.602, β = 1.611, γ = 1.643; $2V_{meas}$ = 56–59(2)° (white light), $2V_{calc}$ = 57 °; *X*^**c** = 10–11°, *Y*^**a** = 10–14°, *Z*^**b** 0–5°. Dispersion of an optical axes is weak, *r* > *v*. A sample used for TG-DTA analysis consisted of a mixture of murakamiite (~71%) and pectolite (~29%) was heated in air from ambient temperature to 1000 °C at a rate of 20 °C/min. The TG-DTA curves show a sharp endotherm at 737 °C followed by 2.80 wt% of weight loss. The averages of chemical analyses [wt% (range)] (16 by LA-ICP-MS/*10 by electron probe*, WDS) are: SiO_2 54.94, (54.52–55.67)/*54.98, (54.47–56.14)*; TiO_2 0.00/*0.01* (0–0.04), Al_2O_3 0.01 (0–0.05)/*0.00*; FeO 0.38 (0.33–0.44)/*0.28 (0.25–0.37)*; MnO 0.80 (0.75–0.85)/*0.56 (0.45–0.68)*, MgO 0.04 (0.03–0.08)/*0.04 (0.01–0.06)*; CaO 34.14 (33.11–34.84)/*33.63 (32.99–34.25)*, Na_2O 4.37 (3.67–5.03)/*4.21 (4.03–4.33)*, Li_2O 2.52 (2.32–2.77)/*2.78* (by LIBS), K_2O 0.00/*0.01 (0–0.03)*, H_2O (by TG-DTA) 2.80; total 100.00 (LA-ICP-MS data normalized to 97.2 wt% excluding H_2O content)/*99.30*. The empirical formulae based on 9 O pfu, are accordingly $(Li_{0.55}Na_{0.46})_{\Sigma1.01}(Ca_{1.98}Mn_{0.03}Fe_{0.02})_{\Sigma2.04}Si_{2.98}O_8(OH)_{1.01}$/*$(Li_{0.61}Na_{0.44})_{\Sigma1.05}(Ca_{1.96}Mn_{0.04}Fe_{0.01})_{\Sigma2.01}Si_{2.99}O_8(OH)_{1.01}$*. The strongest lines in the X-ray powder diffraction pattern are [*d* Å (*I*%; *hkl*)]: 2.897 (100; $2\bar{2}0$), 3.055 (49; 012,102,$1\bar{1}\,\bar{2}$), 3.295 (41; $10\bar{2}$), 3.225 (33; 201), 3.845 (20; 200), 2.284 (19; $10\bar{3}$), 2.720 (15; $12\bar{1}$, $2\bar{2}1$, $20\bar{2}$), 6.962 (15; 001). The unit-cell dimensions refined from the powder data are: *a* = 7.908(2), *b* = 7.031(2), *c* = 6.987 Å, α = 90.48(1), β = 95.558(7), γ = 102.62(1)°, *V* = 377.1 Å^3. Single-crystal X-ray data shows murakamiite is triclinic, space group $P\bar{1}$, *a* = 7.9098(2), *b* = 7.0320(2), *c* = 6.9863(2) Å, α = 90.596(2), β = 95.589(2), γ = 102.767(2)°, *V* = 376.98 Å^3, *Z* = 2. The crystal structure was refined to R_1 =3.28%. It is a pyroxenoid type structure with three-periodic chains of SiO_4 tetrahedra, chains of *M*1 and *M*2 octahedra occupied by Ca and *M*3 polyhedra occupied by Li and Na. The high Li content at *M*3 modifies the arrangement of O atoms defining the *M*3 polyhedra not as eightfold coordinated, but with a distorted sixfold coordination. Murakamiite is a new member of the group of H-bearing Dreierketten pyroxenoids, along with pectolite $NaCa_2Si_3O_8(OH)$, serandite $NaMn_2Si_3O_8(OH)$, tanohataite $LiMn_2Si_3O_8(OH)$ and marshallsussmanite $NaCaMnSi_3O_8(OH)$, an ordered (CaMn) intermediate member of the pectolite–serandite series. The name honored the late Professor Emeritus Nobuhide Murakami (1923–1994) of Yamaguchi University, Japan for his outstanding contributions to petrology and mineralogy, particular the discovery of sugilite and katayamalite in albitites of Iwagi Islet. Type specimens are deposited in the National Museum of Nature and Science, Tsukuba, Japan, and the Geological and Mineralogical Museum of Faculty of Science, Yamaguchi University, Japan. **D.B.**

OXY-FOITITE*

F. Bosi, H. Skogby, and U. Hålenius (2017) Oxy-foitite, □(Fe^{2+}Al$_2$)Al$_6$(Si$_6$O$_{18}$)(BO$_3$)$_3$(OH)$_3$O, a new mineral species of the tourmaline supergroup. European Journal of Mineralogy, 29(5), 889–896.

Oxy-foitite (IMA 2016-069), ideally □(Fe^{2+}Al$_2$)Al$_6$(Si$_6$O$_{18}$)(BO$_3$)$_3$(OH)$_3$O, is a new mineral of the tourmaline supergroup *XY*$_3$*Z*$_6$*T*$_6$O$_{18}$(BO$_3$)$_3$*V*$_3$*W* (Henry et al. 2011) belonging to the X-site vacant group. A hypothetical "oxy-foitite" end-member of the group was proposed by Hawthorne and Henry (1999). The "oxy-foitite" compositions in a natural setting were reported from Vystrčenovice, between Dačice and Telč, Moldanubian, Czech Republic (Povondra 1981; Novák et al. 2004); in the cores of zoned tourmaline grains from quartz veins from the Baraboo Quartzite, Wisconsin, U.S.A. (Medaris et al. 2003) and at Penamacor-Monsanto granite pluton, central eastern Portugal (Ribeiro da Costa et al. 2014). Single-crystal X-ray diffraction, electron microprobe and Mössbauer spectroscopy data for "oxy-foitite" were reported for sample TM84a from Cooma metamorphic Complex, New South Wales, Australia (Bosi and Lucchesi 2004). That sample was further studied in this work followed by oxy-foitite approval by CNMNC IMA. At Cooma Complex the holotype specimen originated from granitic pegmatites in leucosomes and pegmatitic patches occurring in high-grade migmatitic gneisses of pelitic composition. The oxy-foitite formation is related to the partial melting of these gneisses. Associated minerals are muscovite, K-feldspar and quartz. Oxy-foitite forms black, vitreous subhedral prismatic crystals up to ~1 cm striated parallel to [001]. Frequent and evenly distributed micro-fractures in these crystals filled with muscovite and other phases. Crystals are brittle with a gray streak, sub-conchoidal fracture, and no observed cleavage or parting. Mohs hardness is ~7. The density was not measured; D_{calc} = 3.143 g/cm^3. No fluorescence under UV light was observed. In transmitted light, oxy-foitite is pleochroic from pale (E) to dark (O) brown. It is uniaxial (–), ω = 1.660(5), ε = 1.630(5) (white light). Polarized optical absorption spectra in the range 30 000–5000 cm^{-1} on the polished single-crystal fragment show three broad absorption bands caused by electronic 3*d*-transitions: at 22 730 cm^{-1} (440 nm) (Fe^{2+}-Ti^{4+} intervalence charge transfer), 13 990 cm^{-1} (715 nm) and 9090 cm^{-1} (1110 nm) (enhanced spin-allowed *d*–*d* transitions in octahedrally coordinated Fe^{2+}). A number of relatively sharp and weak bands at 7112 (1406 nm), 7092 (1410 nm), and 6959 (1437 nm) cm^{-1} represent overtones of the fundamental (OH)-stretching bands observed at ~3500 cm^{-1}. The (OH) content estimated from the absorbance of the overtone bands in that range indicates 3.0 wt% H_2O in agreement with the chemical data. The polarized FTIR spectra were recorded on the same sample in the range 5000–2000 cm^{-1}. Those recorded parallel to the *c*-axis direction contain a major absorption feature in the 3450–3600 cm^{-1} range being related to the occurrence of (OH) at *V* position. A band at ~ 3375 cm^{-1} is assigned to the hydrogen bond ^{V}O–H···O5. Two sharp bands at 3632 and 3726 cm^{-1} are consistent with the minor concentrations of $^{W}(OH)_{0.39}$ (see empirical formula below). The average of 10 point electron probe analyses [wt% (range)] is SiO_2 (34.95–36.06), TiO_2 0.22 (0.21–0.24), B_2O_3 10.52 (by stoichiometry), Al_2O_3 36.49 (36.29–36.81), FeO_{total} 9.40 (9.07–9.89) (FeO 8.37 and Fe_2O_3 1.15 based on Mössbauer spectroscopy), MgO 2.48 (2.46–2.51), MnO 0.36 (0.32–0.43), ZnO 0.09 (0–0.12), CaO 0.06 (0.05–0.07), Na_2O 1.41 (1.35–1.45), K_2O 0.03 (0.01–0.04), F 0.07 (0–0.15), H_2O (by stoichiometry) 3.08, O=F_2 0.03, total 99.97. The empirical structural formula based on (OH+F+O) = 31 is: $^{X}(\square_{0.53}Na_{0.45}Ca_{0.01}K_{0.01})_{\Sigma1.00}{}^{Y}(Al_{1.53}Fe^{2+}_{1.16}Mg_{0.22}Mn^{2+}_{0.05}Zn_{0.01}Ti^{4+}_{0.03})_{\Sigma3.00}$ $^{Z}(Al_{5.47}Fe^{3+}_{0.14}Mg_{0.39})_{\Sigma6.00}[(Si_{5.89}Al_{0.11})_{\Sigma6.00}O_{18}](BO_3)_3{}^{V}(OH)_3{}^{W}[O_{0.57}F_{0.04}(OH)_{0.39}]_{\Sigma1.00}$. The strongest lines in the X-ray powder diffraction pattern are [*d* Å (*I*%; *hkl*)]: 6.357 (51; 101), 4.220 (47; 211), 3.990 (49; 220), 3.466 (100; 012), 2.953 (122), 2.579 (98; 051), 2.048 (30; 223), 2.041 (50; 152). The cell parameter refined from the X-ray powder data are: *a* = 15.9640(4), *c* = 7.1598(3) Å, *V* = 1580.2 Å^3. The single-crystal X-ray study shows oxy-foitite is trigonal, space group *R*3*m*, *a* = 15.9387(3), *c* = 7.1507(1) Å, *V* = 1573.20 Å^3, *Z* = 3. The crystal structure of oxy-foitite was refined to R_1= 1.48% for 3247 unique reflections. The combination of the chemical, structural, and spectroscopy data is consistent with site population in the empirical structural formula above and the end-member formula □(Fe^{2+}Al$_2$)Al$_6$(Si$_6$O$_{18}$)(BO$_3$)$_3$(OH)$_3$O. The name is given in parallel with the naming of other tourmaline-supergroup species, e.g., oxy-schorl and oxy-dravite, considering that the closest end-member composition among valid tourmaline supergroup species is foitite, ideally □(Fe$^{2+}_2$Al)Al$_6$(Si$_6$O$_{18}$)(BO$_3$)$_3$(OH)$_3$(OH). Oxy-foitite shows chemical relationships with foitite through the substitution ^{Y}Al^{3+} + ^{W}O^{2} → ^{Y}Fe^{2+} + ^{W}(OH)$^{1-}$. The holotype is deposited in the Museum of Earth Sciences, Sapienza University of Rome, Italy. **D.B.**

References cited

Bosi, F., and Lucchesi, S. (2004) Crystal chemistry of the schorldravite series. European Journal of Mineralogy, 16, 335–344.

Hawthorne, F.C., and Henry, D. (1999) Classification of the minerals of the tourmaline group. European Journal of Mineralogy, 11, 201–215.

Henry, D.J., Novák, M., Hawthorne, F.C., Ertl, A., Dutrow, B., Uher, P., and Pezzotta, F. (2011) Nomenclature of the tourmaline supergroup minerals. American Mineralogist, 96, 895–913.

Medaris, L.G., Fournelle, J.H., and Henry, D.J. (2003) Tourmaline-bearing quartz veins in the Baraboo Quartzite, Wisconsin: occurrence and significance of foitite and "oxy-foitite". Canadian Mineralogist, 41, 749–758.

Novák, M., Povondra, P., and Selway, J.B. (2004) Schorl-oxy-schorl to dravite-oxydravite tourmaline from granitic pegmatites; examples from the Moldanubicum, Czech Republic. European Journal of Mineralogy, 16, 323–333.

Povondra, P. (1981) The crystal chemistry of tourmalines of the schorl-dravite series. Acta Universitatis Carolinae, Geologica, 223– 264.

Ribeiro da Costa, M.S., Mourão, C., Récio, C., Guimarães, F., Antunes, I.M., Farinha Ramos, J., Barriga, F.J.A.S., Palmer, M.R., and Milton, J.A. (2014) Tourmaline occurrences within the Penamacor-Monsanto granitic pluton and host-rocks (Central Portugal) genetic implications of crystal-chemical and isotopic features. Contributions to Mineralogy and Petrology, 167, 993.

SHENZHUANGITE*

L. Bindi and X. Xie (2018) Shenzhuangite, $NiFeS_2$, the Ni-analog of chalcopyrite from the Suizhou L6 chondrite. European Journal of Mineralogy, 30(1), 165–169.

Shenzhuangite (IMA 2017-018), $NiFeS_2$, is a new mineral species of chalcopyrite group discovered in the shocked Suizhou L6 chondrite fell on April 15, 1986, in Dayanpo, 12.5 km southeast of Suizhou in Hubei, China. The shock stage classified as S5. Thin shock melt veins less than 300 μm thick contain a number of high-pressure polymorphs including ringwoodite, majorite-pyrope garnet, akimotoite, magnesiowüstite, lingunite, tuite, xieite, hemleyite, and a $(Mg,Fe)SiO_3$-glass—possibly a vitrified perovskite. Shenzhuangite found in a single polished section as unhedral grains up to 60 μm in close association with taenite. Other associated minerals are forsterite, pyroxene, plagioclase glass (maskelynite), and troilite. Color, luster, streak, hardness, tenacity, cleavage, fracture, and density were not determined because of the small grain size; D_{calc} = 4.013 g/cm^3. In plane-polarized incident light, shenzhuangite is yellowish. Under crossed polars, it is weakly anisotropic with light brown to greenish rotation tints. Internal reflections are absent. Reflectance values were measured in air for COM wavelengths [R_1, R_2 (nm)] are: 24.8, 26.0 (471.1); 34.9, 36.2 (548.3); 37.7, 39.1 (586.6); 40.4, 41.1 (652.3). The average of 4 electron-microprobe WDS analyses [wt% (range)] is Ni 22.37 (22.01–23.12), Fe 30.87 (29.85–31.12), Cu 10.88 (10.15–11.27), Co 0.07 (0.02–0.11), S 35.42 (34.98–36.02), total 99.61 wt%. No other elements with $Z > 9$ were detected. The empirical formula based on 4 apfu and assuming the crystal-chemical exchange: $Cu^+ + Fe^{3+} \leftrightarrow Ni^{2+} + Fe^{2+}$ is $(Ni^{2+}_{0.69}Cu^{+}_{0.31})(Fe^{2+}_{0.69}Fe^{3+}_{0.31})_{\Sigma 2.00}$. The strongest X-ray powder-diffraction lines [d Å (I%; hkl)] are: 3.05 (100; 112), 1.875 (20; 220), 1.591 (25; 312,116), 1.215 (10; 332,316), 1.080 (10; 424). The tetragonal unit-cell parameters refined from the power data are: a = 5.3064(2), c = 10.399(3) Å, V = 292.88 Å^3. The single-crystal X-ray data shows tetragonal space group $I\bar{4}2d$, a = 5.3121(4), c = 10.4772(7) Å, V = 295.65 Å^3, Z = 4. The crystal structure was refined to R_1 = 0.0369 for 836 unique reflections and shows shenzhuangite is the Ni-analog of chalcopyrite. It likely formed as alteration of pre-existing taenite when pS_2/pO_2 ratios allowed sulfurization of the FeNi metal. Shenzhuangite is named in honor of Shangyue Shen and Xiaoli Zhuang who first discovered the Ni-rich variety of chalcopyrite in the Suizhou meteorite. Holotype material is deposited in the Museo di Storia Naturale, Università degli Studi di Firenze, Italy. **D.B.**

SIIDRAITE*

M.S. Rumsey, M.D. Welch, A.K. Kleppe, and J. Spratt (2017) Siidraite, $Pb_2Cu(OH)_2I_3$, from Broken Hill, New South Wales, Australia: the third halocuprate(I) mineral. European Journal of Mineralogy, 29(6), 1027–1030.

Siidraite (IMA 2016-038), ideally $Pb_2Cu(OH)_2I_3$, is a new mineral from the classic Broken Hill deposit in New South Wales, Australia. It was discovered on a single specimen BM 84642 registered as marshite at the Natural History Museum, London, obtained from the mineral dealer A.E. Foote of Philadelphia in 1899. Specific locality within the deposit is unknown. This specimen is now considered as holotype of siidraite along with the polished probe block and single-crystal mount removed from it. The specimen is a mass of cuprite and native copper, with cavities incrusted by well-formed cuprite octahedra with a small relict blebs and broken shards of the characteristic Broken Hill galena–Mn-silicate ore and quartz. Some cavities contain a suite of secondary minerals: orange/pale-brown translucent marshite tetrahedra (dominated), linarite, connellite, brochantite, tsumebite, anglesite, plumbogummite-group minerals (traces), and occasionally, tiny yellow granular aggregates of the siidraite. It is suggested that siidraite formed from the secondary alteration of cuprite due to the local availability of Pb mobilized from the small galena "blebs" and shards at the contacts with cuprite. Siidraite forms patches up to 2 mm, although individual crystal aggregates are up to 0.3 mm across with the largest single crystal of 0.1 mm long. It is yellow and translucent with a yellow streak, has vitreous luster and no parting or cleavage. Siidraite is non-fluorescent in mixed-wavelength UV light. Crystal forms are indistinct. Due to the crystal size and the scarcity of the material the Mohs hardness (estimated as ~2½–3½), density (D_{calc} = 6.505 g/cm^3), optical properties (n_{calc} = 2.18), and X-ray powder diffraction data were not obtained. The Raman spectrum shows peaks below 400 cm^{-1} attributed to modes of the cubane group $[Pb_4(OH)_4]$ and Cu_2I_6 dimer units, and internal modes of the CuI_4 tetrahedra, and peaks at 3443 and 3455 cm^{-1} attributed to two non-equivalent OH groups. The average of 10 electron probe WDS analyses is [wt% (range)]: Cu_2O 7.22 (6.96–7.35), PbO 51.8 (50.1–53.4), I 42.5 (42.2–42.8), H_2O (by stoichiometry) 2.03 (1.99–2.08), –(OH)=I 2.61, total 100.94. The empirical formula based on 5 anions pfu is $Pb_{2.06}Cu_{0.89}(OH)_2I_{2.97}$. The strongest lines in the calculated X-ray powder-diffraction pattern [d_{calc} Å (I_{calc}%; hkl)] are: 2.746 (100; 246), 3.270 (81; 404), 2.738 (77; 264), 3.312 (76; 315), 3.296 (69; 351). Single-crystal X-ray diffraction data refined to R_1 = 0.037 for 1368 unique $I \geq 2\sigma(I)$ reflections shows siidraite is orthorhombic, space group $Fddd$, a = 16.7082(9), b = 20.846(1), c = 21.016(1) Å, V = 7320.0 Å$_3$, Z = 32. The structure of siidraite consists of a framework that involves alternation of two structural elements, a cubane-like $[Pb_4(OH)_4]^{4+}$ group and a $[Cu_2I_6]^{4-}$ dimer of edge-sharing CuI_4 tetrahedra. Six halocuprate groups surround each $[Pb_4(OH)_4]^{4+}$ nucleus, and each halocuprate group is shared between six adjacent $[Pb_4(OH)_4]^{4+}$ groups. Long Pb–I bonds complete the coordination of each Pb atom resulting in $Pb(OH)_3I_5$ polyhedra centred on a tetrahedron of O atoms to form a $Pb_4(OH)_4I_{16}$ cluster. Siidraite is named after Russian mineralogist and crystallographer Oleg. I. Siidra (b. 1981) for his extensive work on secondary lead oxysalts and, in particular, on synthetic iodine-rich phases. **O.C.G.**

ULFANDERSSONITE-(CE)

D. Holstam, L. Bindi, U. Hålenius, U. Kolitsch, and J. Mansfeld (2017) Ulfanderssonite-(Ce), a new Cl-bearing REE silicate mineral species from the Malmkärra mine, Norberg, Sweden European Journal of Mineralogy, 29(6), 1015–1026.

Ulfanderssonite-(Ce) (IMA 2016-107), ideally $Ce_{15}CaMg_2(SiO_4)_{10}(SiO_3OH)(OH,F)_5Cl_3$, monoclinic, is a new mineral discovered at the long-abandoned Malmkärra iron mine, one of the Bastnäs-type Fe-REE deposits in the Bergslagen ore region, central Sweden. These deposits, comprising REE silicates and fluorocarbonates in association with magnetite and Mg silicates are metasomatic skarn

mineralization, formed by fluids rich in REEs and other metals that have reacted with carbonate layers in the volcano-sedimentary pile. More than 20 REE minerals have been reported from the area. The new mineral discovered in the specimen collected in 1986 from mine dumps and originally catalogued as cerite-(Ce) with allanite-(Ce) in the Mineralogical Museum of Uppsala University, under the number 318/77. The specimen appeared to be consisted mainly of västmanlandite-(Ce) and a new mineral—ulfanderssonite-(Ce). The similar mineral was previously mentioned as unnamed "mineral E" (Holtstam and Andersson 2007), which is reported as UM2007-39 in the official list of valid unnamed mineral species (Smith and Nickel 2007). Ca- and Cl-rich REE-silicate intergrown with fluorbritholite-(Ce) from Malmkärra was noted by Sahlström (2014) with no more detailed information. The grains with composition very similar to that of ulfanderssonite-(Ce) (with Fe > Mn) were found in contact with cerite-(Ce) at the Nya Bastnäs ore field, ~30 km to the SSW of the Malmkärra mine (Holtstam and Andersson 2007). That may represent an unnamed Fe analog of ulfanderssonite-(Ce). The "Cl- and F-rich cerite-(Ce)" from the Crosetto talc mine, Germanasca valley, Torino Province, Italy (Piccoli et al. 2007; Chukanov 2014) may be closely related to ulfanderssonite-(Ce) based also on similarity of IR spectra. The type specimen ulfanderssonite-(Ce) is associated with västmanlandite-(Ce), bastnäsite-(Ce), phlogopite, talc, magnetite, pyrite, fluorbritholite-(Ce), and scheelite. Alteration to bastnäsite-(Ce) and other unidentified fluoro-carbonates locally occurs along grain boundaries and micro-cracks. The mineral forms pinkish, translucent subhedral grains, 100–300 mm, in flesh-pink to colorless-gray vitreous to greasy aggregates up to 2 mm. It is non-fluorescent under UV radiation. The streak is white. The indistinct cleavage is on (001); fracture is uneven. Ulfanderssonite-(Ce) is brittle with Mohs hardness 5–6. The density was not measured due to impurities; D_{calc} = 4.97 g/cm^3. In transmitted light ulfanderssonite-(Ce) is nearly colorless, non-pleochroic, has a slight undulatory extinction. It is optically biaxial (–), $2V_{meas}$ = 55°. The refractive indexes were not measured (n > 1.81); n_{calc} = 1.82. An unpolarized single-crystal FTIR-spectrum in the range 600–5000 cm^{-1} shows broad band features at ~2850 and ~3250 cm^{-1}, and relatively sharp bands at 3400, 3510, and 3635 cm^{-1} (O–H stretching vibrations); very intense absorption in the range 800–1050 cm^{-1} (SiO_4 modes); 2140 and ~2330 cm^{-1} (lattice combination modes). No bands attributable to CO_3^{2-} or H_2O groups were observed. The average of 10 electron probe WDS analyses is [wt% (range)]: La_2O_3 11.87 (11.28–12.45), Ce_2O_3 30.98 (29.66–31.83), Pr_2O_3 3.99 (3.78–4.20), Nd_2O_3 17.14 (16.68–17.64), Sm_2O_3 2.81 (2.60–3.13), Eu_2O_3 0.18 (by LA-ICP-MS), Gd_2O_3 1.15 (0.84–1.48), Dy_2O_3 0.30 (0.22–0.42), Tb_2O_3 0.10 (by LA-ICP-MS), Y_2O_3 1.11 (0.82–1.45), CaO 2.26 (2.02–2.51), FeO 0.02 (0–0.08), MgO 1.97 (1.90–2.10), P_2O_5 0.08 (0–0.28), SiO_2 19.13 (18.47–19.47), H_2O_{calc} 1.07 (based on OH+F+Cl = 9 pfu), F 1.09 (0.93–1.25), Cl 2.89 (2.85–2.97), O=F –0.46, O=Cl –0.64, total 97.04. Elements Na, K, Sr, Ba, Al, Mn, and Ti were below detection limits. LA-ICP-MS analyses show the presence of Ho, Er, Tm, Yb, Lu, Bi, Cu, W, U, and Th in trace amounts. No specific explanation for the low totals found beside a partial sample degradation under the electron beam. The empirical formula calculated on the basis of 29 cations pfu, is $(Ce_{6.58}Nd_{3.55}La_{2.54}Pr_{0.84}Sm_{0.56}Y_{0.34}Gd_{0.22}Dy_{0.06}Eu_{0.04}Tb_{0.02}Ca_{1.41})_{\Sigma 16.16}Mg_{1.70}Fe_{0.01}Si_{11.11}P_{0.04}O_{43}(OH)_{4.16}F_{2.00}Cl_{2.84}$. The strongest lines in the X-ray powder-diffraction pattern [d (Å) (I%; hkl)] are: 4.350 (21; 022), 3.524 (26; 401), 2.948 (100; 421), 2.923 (47; 204), 2.683 (24; 040), 2.660 (32; 225), 1.760 (25; 623). The monoclinic unit-cell parameters, refined from the powder data are a = 14.140(2), b = 10.740(2), c = 15.506(2) Å, β = 106.64(2)°, V = 2256.2 Å^3. Single-crystal X-ray data shows ulfanderssonite-(Ce) is monoclinic, Cm, with a = 14.1403(8), b = 10.7430(7), c = 15.498(1) Å, β = 106.615(6)°, V = 2256.0 Å^3 for Z = 2. The crystal structure has been solved by direct methods and refined to R_1 = 2.97% for 5280 observed $F_o > 4\sigma(F_o)$ reflections. The basic structural elements of ulfanderssonite-(Ce) are 11 distorted $(REE,Ca)O_{7-9}Cl_{0-2}$ polyhedra, 2 regular MgO_6 octahedra, and 7 SiO_4 tetrahedra (one of which is protonated). Although strictly not a layer topology, the crystal structure can be described as a regular alternation of the two kinds of layers alternated along the c-axis. The layer with composition $[(Ce_8Ca)MgSi_7O_{22}(OH,F)_4]^{8+}$ (~9 Å thick) is topologically and chemically closely related to cerite-(Ce). The layer with composition $[Ce_7MgSi_4O_{21}(OH,F)_2Cl_3]^{8-}$ (~6.5 Å thick) has a novel topology. Ulfanderssonite-(Ce) along with fluorbritholite-(Ce) are interpreted as primary minerals formed by a magmatic-hydrothermal fluid with REE, Si, F, and Cl ion complexes reacting with dolomite marble. The presence of ulfanderssonite-(Ce) is direct evidence of a Cl-rich mineral-forming aqueous solution, normally not reflected in the composition of skarn minerals in Bastnäs-type deposits. The mineral name honors Ulf B. Andersson, a Swedish geologist and petrologist contributed significantly to the understanding of the Bastnäs deposits genesis. The holotype material, including a polished thin section, is deposited in the, Swedish Museum of Natural History. **D.B.**

References cited

Chukanov, N.V. (2014) Infrared Spectra of Mineral Species. Extended library. Springer, 1726 p.

Holtstam, D., and Andersson, U.B. (2007) The REE minerals of the Bastnäs-type deposits, South-Central Sweden. Canadian Mineralogist, 45, 1073–1114.

Piccoli, G.C., Maletto, G., Bosio, P., and Lombardo, B. (2007) Minerali del Piemonte e della Valle d'Aosta. Associazione Amici del Museo "F. Eusebio", Alba, Ed., Alba (Cuneo), 607.

Sahlström, F. (2014) Stable isotope systematics of skarn-hosted REE silicate-magnetite mineralisations in central Bergslagen, Sweden. M.Sc. thesis, Department of Earth Sciences, Uppsala University, 83 p.

Smith, D.G.W., and Nickel, E.H. (2007) A system for codification for unnamed minerals: report of the Subcommittee for Unnamed Minerals of the IMA Commission on New Minerals, Nomenclature and Classification. Canadian Mineralogist, 45, 983–1055.

American Mineralogist is now available online three ways

▼1 ***Via MSA*** – The classic PDF presentation in a simple no-frills environment. To view: http://www.minsocam.org/msa/ammin/toc/. *Institutional Subscription information:* http://www.minsocam.org/msa/AmMin/subscription.html

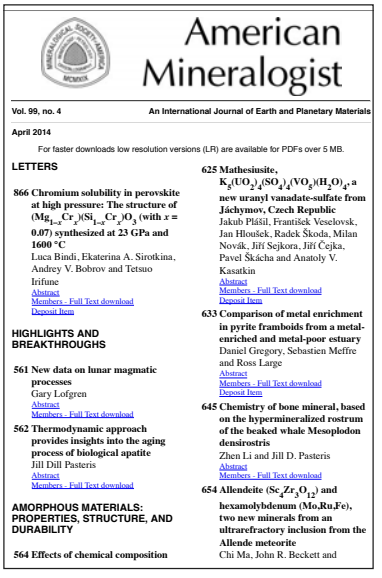

American Mineralogist

Vol. 99, no. 4 — An International Journal of Earth and Planetary Materials

April 2014

For faster downloads low resolution versions (LR) are available for PDFs over 5 MB.

LETTERS

866 Chromium solubility in perovskite at high pressure: The structure of $(Mg_{1-x}Cr_x)(Si_{1-x}Cr_x)O_3$ (with x = 0.07) synthesized at 23 GPa and 1600 °C
Luca Bindi, Ekaterina A. Sirotkina, Andrey V. Bobrov and Tetsuo Irifune
Abstract
Members - Full Text download
Deposit Item

HIGHLIGHTS AND BREAKTHROUGHS

561 New data on lunar magmatic processes
Gary Lofgren
Abstract
Members - Full Text download

562 Thermodynamic approach provides insights into the aging process of biological apatite
Jill Dill Pasteris
Abstract
Members - Full Text download

AMORPHOUS MATERIALS: PROPERTIES, STRUCTURE, AND DURABILITY

564 Effects of chemical composition

625 Mathesiusite, $K_5(UO_2)_4(SO_4)_4(VO_5)(H_2O)_4$, a new uranyl vanadate-sulfate from Jáchymov, Czech Republic
Jakub Plášil, František Veselovsk, Jan Hloušek, Radek Škoda, Milan Novák, Jiří Sejkora, Jiří Čejka, Pavel Škácha and Anatoly V. Kasatkin
Abstract
Members - Full Text download
Deposit Item

633 Comparison of metal enrichment in pyrite framboids from a metal-enriched and metal-poor estuary
Daniel Gregory, Sebastien Meffre and Ross Large
Abstract
Members - Full Text download
Deposit Item

645 Chemistry of bone mineral, based on the hypermineralized rostrum of the beaked whale Mesoplodon densirostris
Zhen Li and Jill D. Pasteris
Abstract
Members - Full Text download

654 Allendeite ($Sc_4Zr_3O_{12}$) and hexamolybdenum (Mo_6Ru_2Fe), two new minerals from an ultrarefractory inclusion from the Allende meteorite
Chi Ma, John R. Beckett and

►2 ***Via Geoscienceworld*** – Since 2004, a comprehensive Internet resource for research across the geosciences, built on a database of peer-reviewed journals and integrated with GeoRef, enhanced with specialized tools developed in partnership with Google Maps™. This gives global researchers a single point of access to 45 full-text scholarly journals and links to millions of relevant resources hosted elsewhere on the Web. http://ammin.geoscienceworld.org/. Many features, html and PDF views. *To subscribe:* http://www.geoscienceworld.org/site/subscriptions/

New data on lunar magmatic processes
Gary Lofgren
American Mineralogist April 01, 2014, Vol.99, 561, doi:10.2138/am.2014.4803

Thermodynamic approach provides insights into the aging process of biological apatite
Jill Dill Pasteris
American Mineralogist April 01, 2014, Vol.99, 562-563, doi:10.2138/am.2014.4860

Effects of chemical composition and temperature on transport properties of silica-rich glasses and melts
Supplementary data
American Mineralogist April 01, 2014, Vol.99, 564-577, doi:10.2138/am.2014.4683

Speciation of and D/H partitioning between fluids and melts in silicate-D-O-H-C-N systems determined in-situ at upper mantle temperatures, pressures, and redox conditions
American Mineralogist April 01, 2014, Vol.99, 578-588, doi:10.2138/am.2014.4575

Effect of oxalate and pH on chrysotile dissolution at 25 °C: An experimental study
Supplementary data
American Mineralogist April 01, 2014, Vol.99, 589-600, doi:10.2138/am.2014.4636

◄3 ***Via De Gruyter*** – our newest offering, another way for libraries to reach out and include the best articles and the greatest variety of Earth Science for its size. Many of the features you expect in today's web, such as eTOC alerts and new article alerts and cite/export. Articles are presented in downloaded PDF format. *To subscribe:* http://www.degruyter.com/view/j/ammin

Our Aims and Scope

American Mineralogist: Journal of Earth and Planetary Materials, is the flagship journal of the Mineralogical Society of America (MSA), continuously published since 1916. Our mission is to provide readers with reports on original scientific research, both fundamental and applied, with far reaching implications and far ranging appeal. Topics of interest cover all aspects of planetary evolution, and biological and atmospheric processes mediated by solid-state phenomena. These include, but are not limited to, mineralogy and crystallography, high- and low-temperature geochemistry, petrology, geofluids, bio-geochemistry, bio-mineralogy, synthetic materials of relevance to the Earth and planetary sciences, and breakthroughs in analytical methods of any of the aforementioned.

Have your librarian pick the one that suits your institution's needs and budget today!